Rapid sample-saving biophysical characterization and long-term storage stability of liquid interferon alpha2a formulations: Is there a correlation?

Hristo Svilenov, Gerhard Winter

PII: S0378-5173(19)30211-X
DOI: https://doi.org/10.1016/j.ijpharm.2019.03.025
Reference: IJP 18209

To appear in: *International Journal of Pharmaceutics*

Received Date: 18 December 2018
Revised Date: 10 March 2019
Accepted Date: 11 March 2019

Please cite this article as: H. Svilenov, G. Winter, Rapid sample-saving biophysical characterization and long-term storage stability of liquid interferon alpha2a formulations: Is there a correlation?, *International Journal of Pharmaceutics* (2019), doi: https://doi.org/10.1016/j.ijpharm.2019.03.025

Rapid sample-saving biophysical characterization and long-term storage stability of liquid interferon alpha2a formulations: Is there a correlation?

Hristo Svilenov†, Gerhard Winter

Department of Pharmacy, Pharmaceutical Technology and Biopharmaceutics, Ludwig-Maximilians-University, Butenandtstrasse 5-13, Munich D-81377, Germany

†Corresponding author: hrisph@cup.uni-muenchen.de

Abstract

The knowledge and tools to characterize proteins have comprehensively developed in the last two decades. Some of these tools are used in formulation development to select formulation conditions suitable for long-term storage. However, there is an ongoing debate whether the predictions obtained with these tools are in a good agreement with the outcome from real-time long-term stability studies. In this work, we investigate whether some of the state-of-the-art microscale, microvolume and non-destructive biophysical techniques can be applied to promptly select formulations that minimize the aggregation of interferon alpha2a during storage. Interferon alpha2a was used as a model protein as it is known to form aggregates at concentrations over an order of magnitude higher than used in the commercial product. We apply a systematic formulation approach in which we investigate the effect of pH and ionic strength on protein stability. The predictions from the sample-saving biophysical characterization are validated by long-term stability studies at 4 ^{o}C and 25 ^{o}C for 12 months on selected formulations. Interferon alpha2a shows minimal aggregation in 10 mM sodium acetate buffer with pH 4 and low ionic strength. The latter is indicated by the rapid sample-saving biophysical characterization and confirmed by the long-term stability data.

Keywords

Protein stability; Protein Formulation; Protein Aggregation; Therapeutic proteins; Protein storage stability; High-throughput protein characterization;

Abbreviations

ACF – autocorrelation function from dynamic light scattering data evaluation;

DLS – dynamic light scattering;

GuHCl – guanidine hydrochloride;

HP-SEC – size exclusion chromatography;

ICD – isothermal chemical denaturation;

IFNα2a – recombinant interferon alpha2a;

$IP_{350/330}$ – Inflection point of the protein unfolding transition detected by the integrated intrinsic fluorescence intensity ratio (FI350nm/FI330nm);

RP-HPLC – reversed-phase chromatography;

T_{agg} – protein aggregation onset temperature from the aggregation detection optics of the Prometheus® NT.48;

T_{on} – protein aggregation onset temperature from the increase in the protein hydrodynamic radius measured by dynamic light scattering;

1. Introduction

The introduction of the first biologics to the market more than three decades ago has revolutionised the therapy of many severe diseases (Revers and Furczon, 2010). Unfortunately, this new type of medicines brought not only benefits to the patients and the pharmaceutical companies but also many new challenges related to their development, production and safety. One typical hurdle of biologics, in particular of protein-based drugs, is the tendency of proteins to form aggregates of various sizes and characteristics (Narhi et al., 2012; Roberts, 2007; Roberts et al., 2011; Smith et al., 2010). On the one hand, the formation of large aggregates during the shelf-life of a medicine can lead to non-compliance with the tight regulatory limits for subvisible and visible particles in parenteral drugs. On the other hand, the protein aggregates are considered degradation products according to the ICH guidelines and their presence has been related to undesired immunogenic reactions in patients (*ICH, Q5C Quality of Biotechnological Products: Stability Testing of Biotechnological/Biological Products*, 1995; Moussa et al., 2016; Ratanji et al., 2014; Rosenberg, 2006). The above-mentioned reasons require the adoption of different strategies to minimize the presence and formation of protein aggregates in parenteral drugs. One often-used strategy is the selection of formulation conditions (e.g. pH, ionic strength) that impede aggregate formation and growth during storage (Wang and Roberts, 2018). One approach to select the optimal formulation conditions for a protein would be to prepare dozens of different samples and store them at the temperature of interest (e.g. 4 ^{o}C) for 1-2 years to see which of them are the most stable. This approach is impractical for both time and sample-consumption reasons. A second approach would be to perform accelerated stability and stress studies (e.g. at 25 ^{o}C and 40 ^{o}C) for a few weeks/months to select only the most promising formulations that will move on to long-term stability testing. This approach, similar to the first one, is also related to a large sample consumption and a significant analytical effort. A third approach, that has been explored by academia and industry for over two decades, is to use biophysical techniques that provide data which can facilitate the selection of promising formulation conditions (E. Y. Chi et al., 2003; Manning et al., 2018). The working principles of the techniques used in the third approach have not changed significantly over the years and most methods rely on fluorescence or light scattering measurements. Most efforts to improve these methods have been aimed at creating label-free techniques, improving data quality and reproducibility, as well as reducing the sample amounts required for measurements and adapting the methods for automation. Still, there is an ongoing debate if and to what extent the data obtained from these methods is predictive for the stability of the proteins during long-term storage (Brader et al., 2015; Goldberg et al., 2017; Robinson et al., 2018).

Interferon alpha2a (IFNα2a) is a classic example of a protein-based parenteral drug. IFNα2a gained first approval by the FDA in the mid-80s and is used to treat patients suffering from different types of

hepatitis, carcinoma, leukemia, lymphoma and several other conditions(Baron et al., 1991; Dragomiretskaya et al., 2015; Escudier et al., 2007; Jonasch and Haluska, 2001). The benefit of IFNα2a therapy has been repeatedly proven in various clinical trials. However, IFNα2a is a protein which is prone to form aggregates and the presence of the latter, when formulated with HSA or chemically cross-linked, has been linked to undesired immunogenic reactions in mouse models and human patients (Braun et al., 1997; Hochuli, 1997). Some of these issues led to changes in the formulation, removing HSA, of IFNα2a in the mid-90s(Hochuli, 1997; "US5762923A - Stabilized interferon alpha solutions - Google Patents," n.d.). More recent work on aggregates and immunogenicity suggests the need for chemical modification, not simply aggregation, to drive immunogenicity to therapeutic proteins(Bessa et al., 2015; Boll et al., 2017). Still, the goal during the formulation development is to find conditions that suppress the formation of protein aggregates of any origin. Noteworthy, IFNα2a was developed and characterized in times when the available techniques for protein formulation and analysis were limited in comparison to the tools we have nowadays.

Our goal in this work is to investigate whether some of the modern rapid sample-saving techniques can be used to promptly obtain stability-indicating data that can be reliably used in formulation development. To do so, we apply a systematic formulation approach, which includes three steps: Step 1 - Screen for optimal pH; Step 2 - Screen for the effect of ionic strength (i.e. sodium chloride) on the protein stability; Step 3 - Advanced structural characterization; Finally, we study the long-term stability of IFNα2a in different formulations after storage at 4 °C and 25 °C to validate the predictions from the rapid, sample-saving biophysical characterization. This work shows how the techniques we explore can be integrated into a quick and systematic (pre-)formulation approach which successfully found a liquid interferon alpha2a formulation that is stable during long-term storage.

2. Materials and methods

2.1. Materials

Interferon alpha2a was kindly provided by Roche Diagnostics GmbH, Penzberg, Germany. The bulk solution contains 1.35 g/L protein, 25 mM ammonium acetate buffer with pH 5 and 120 mM sodium chloride. The protein concentration was measured spectrophotometrically using the NanoDrop 2000 (Thermo Fisher Scientific, Wilmington, USA) and an $A280_{0,1\%} = 0.972$. All other chemicals were obtained from Sigma-Aldrich. All solutions were prepared with ultrapure water from a Sartorius arium® pro system. All buffers used in this work had a concentration of 10 mM and were prepared by combining the respective amounts of the 10 mM free acid and 10 mM free base stock solutions with no subsequent pH adjustment. The pH after preparation was ±0.1 of the target value. Important to note, the protein concentration 1 g/L that we used is higher than the concentration in the commercially

available products with IFNα2a. Our aim was not to compare the stability of our formulations to the commercial products but to use IFNα2a as a model protein for our studies.

2.2. Sample dialysis and preparation

2.2.1. Screen for the effect of pH (Step 1)

The buffer of interferon alpha2a for the first formulation step was exchanged in the following way – the IFNα2a bulk solution was diluted to 1 g/L and 100 µL aliquots were filled in Pierce™ microdialysis devices with a membrane having 3.5 kDa MWCO. The samples were dialyzed at 25 ^{o}C against 1.6 mL of buffer (10 mM sodium acetate with pH 3.5, 4.0, 4.5, 5.0 or 5.5; or 10 mM sodium phosphate with pH 6.0, 6.5, 7.0, 7.5 or 8.0). The buffer was exchanged every two hours (5 exchanges in total) to ensure a constant concentration gradient across the dialysis membrane. After the last change, the samples were left to dialyse overnight. Finally, the samples were collected in microcentrifuge tubes and centrifuged at 10.000 x g for 10 minutes. The following measurements were performed on the supernatant.

2.2.2. Screen for the effect of sodium chloride (Step 2)

Few millilitres of IFNα2a bulk solution were filled in Spectra/Por® 6-8 kDa MWCO dialysis tubing (Spectrum Laboratories Inc., Rancho Dominguez, USA) and dialyzed at 20 – 25 °C against excess (approximately 1:200) of 10 mM sodium acetate buffer with pH 4 or 5. Two buffer exchanges were performed 3 and 8 hours after the beginning. After the last change, dialysis was continued for another 16 hours. Stock solutions of sodium chloride (10X) were prepared in the respective buffer and spiked into the dialyzed IFNα2a to prepare samples containing 1 g/L protein in 10 mM sodium acetate with pH 4 or 5 and varying concentrations of sodium chloride.

2.2.3. Advanced Protein Characterisation (Step 3) and Long-Term Stability Study

The IFNα2a buffer was exchanged and sodium chloride was spiked in the samples to a final concentration of 70 mM as described in 2.2.2. Subsequently, the samples were sterile filtered with 0.22 µm cellulose acetate filter. For the long-term stability study, the solutions were aseptically filled into pre-sterilized DIN2R glass type I vials (2 mL solution in each vial). Finally, the vials were crimped with rubber stoppers and stored at 4 ^{o}C and 25 ^{o}C. At each time point (i.e. 0, 3, 6, 9 and 12 months for the storage at 25 ^{o}C; and 0, 6 and 12 months for the storage at 4 ^{o}C), three new different vials were opened and used for the analysis of every condition.

2.3. High-throughput Fluorimetric Analysis of Thermal Protein Unfolding with nanoDSF®

nanoDSF® was used to study the protein thermal unfolding and aggregation (Linke et al., 2016; Wanner et al., 2017). The IFNα2a solutions were filled into standard glass capillaries (NanoTemper Technologies, Munich, Germany) and placed in the Prometheus® NT.48 (NanoTemper Technologies, Munich, Germany). A temperature ramp of 1 °C/min was applied from 20 to 95°C. All measurements were performed in triplicates. The Prometheus® NT.48 system measures the integrated intrinsic protein fluorescence intensity at 330 and 350 nm after excitation at 280 nm in each capillary. Simultaneously, the system can detect aggregation/precipitation of the samples with a detector which measures the back-reflection intensity of a light beam that passes twice through the capillary(Söltl et al., 2015). The fluorescence intensity ratio (F350/F330) was plotted against the temperature and the inflection point ($IP_{350/330}$) of the transition was derived from the maximum of the first derivative of each measurement using the PR.ThermControl V2.1 software (NanoTemper Technologies, Munich, Germany). In addition, the aggregation onset temperature (T_{agg}) from the increase in the signal from the aggregation detection optics was determined using the same software.

2.4. Dynamic Light Scattering (DLS) in Micro Well Plates

Five µL of IFNα2a solution were filled in 1536 well LoBase plate (Aurora Microplates Inc., Carlsbad, USA) and the plate was centrifuged at 2200 rpm for 2 minutes using a Heraeus Megafuge 40 centrifuge equipped with an M-20 well plate rotor (Thermo Fisher Scientific, Wilmington, USA). Next, each well was sealed with 5 µl of silicon oil and centrifuged again at 2200 rpm for 2 minutes. The well plate was placed in a DynaPro® DLS plate reader (Wyatt Technology Europe, Dernbach, Germany) and 10 acquisitions of 5 seconds at 25 ^{o}C were collected for each sample. The autocorrelation function (ACF) of each sample was calculated from the fluctuation of the light scattering intensity using the Dynamics V7.8 software. Cumulant analysis was performed with the same software to derive the apparent coefficient of self-diffusion (D) and the polydispersity index (PDI). Next, the apparent protein hydrodynamic radius from DLS (R_h) was calculated using the Stokes-Einstein equation using the viscosity of the respective sample. The viscosity of the samples was calculated using the solvent tool of the Zetasizer software (Malvern, Herrenberg, Germany). Additionally, the viscosity of some control samples was measured experimentally with a falling ball viscometer. In all cases, the viscosity of the solutions was ±2 % of the viscosity of pure water. More data on the viscosity of the solution and its effect on the calculated R_h can be found in Supplementary data (Fig S4). For the temperature ramp experiments, 5 acquisitions of 5 seconds were taken while a temperature ramp of 0.1 °C/min was applied from 25 to 80 °C. The aggregation onset temperature (T_{on}) from the increase in the R_h from DLS was determined using the Dynamics V7.8 software. All measurements were performed in triplicates.

2.5. Microscale Isothermal Chemical Denaturation (ICD)

Stock solutions of IFNα2a, buffer and 7 M guanidine hydrochloride (GuHCl) in the respective buffer were combined in a non-binding surface 384 well plate (Corning, USA) with the Viaflo Assist system (Integra Biosciences, Konstanz, Germany) as earlier described(Svilenov et al., 2018). Next, the samples are incubated for 1 hour at room temperature, filled into standard nanoDSF® glass capillaries and the integrated intrinsic protein fluorescence at 330 and 350 nm was measured with the Prometheus® NT.48. The ratio F350/330 was plotted against the denaturant concentration and the curve was fit to a two-state protein unfolding model using the PR.ChemControl V1.4.2 software (NanoTemper Technologies, Munich, Germany) to obtain the Gibbs free energy of unfolding (ΔG), the melting denaturant concentration (C_m) and the m-value. The experiment was performed in triplicates.

2.6. Circular dichroism (CD)

Near- and far-UV circular dichroic spectra of IFNα2a solutions with a concentration of 1 g/L were collected at 25 °C with a Jasco J-810 spectropolarimeter (JASCO Deutschland GmbH, Pfungstadt, Germany). Quartz cuvettes with 10 mm and 0,1 mm wavelength path were used for the near-UV and the far-UV measurements respectively. 10 accumulations of each sample were taken with a speed of 20 nm/min. The spectrum of the respective buffer was subtracted for each sample, the spectra were smoothed using Savitzky-Golay algorithm with 7 smoothing points(Savitzky and E, 1951) and the mean residue ellipticity was calculated as described elsewhere(Towsend et al., 1967).

2.7. Fourier-transform Infrared Spectroscopy (FT-IR)

FT-IR spectra of IFNα2a solutions with a concentration of 1 g/L were collected using a Tensor 27 (Bruker Optik GmbH, Ettlingen, Germany) equipped with a BioATR (Attenuated Total Reflectance) cell™ II (Harrick) at 25 °C connected to a thermostat (DC30-K20, Thermo Haake). 120 scans with a resolution of 4 cm^{-1} were used to obtain each spectrum. The data was further analysed with Opus 7.5 (Bruker Optik GmbH) software and presented as a vector-normalized second-derivative spectrum. The data was smoothed using a Savitzky-Golay algorithm with 17 smoothing points(Savitzky and E, 1951).

2.8. Size Exclusion Chromatography (HP-SEC)

A Dionex Summit 2 system (Thermo Fisher, Dreieich, Germany) was used for the size exclusion chromatography. 25 µg of IFNα2a were injected on a TSKgel G3000SWxl, 7,8x300 mm, 5 µm column (Tosoh Bioscience, Tokyo, Japan) and the elution of the protein was detected at 343 nm after excitation at 280 nm with an RF2000 fluorescence detector (Thermo Fisher, Dreieich, Germany). The fluorescence

detection to detect IFNα2a aggregates with HP-SEC is already successfully used by other groups(Diress et al., 2010). The running buffer consisted of 50 mM sodium acetate pH 5 with 500 mM arginine hydrochloride. The chromatograms were integrated in Chromeleon V7 (Thermo Fisher, Dreieich, Germany) and the relative area of the high molecular species (i.e. small soluble aggregates) was calculated in percentage.

2.9. Flow Imaging Microscopy (FlowCAM)

The IFNα2a samples on long-term stability study were analysed for the presence of larger protein aggregates (subvisible particles) with a FlowCAM® 8100 (Fluid Imaging Technologies, Inc., Scarborough, ME, USA). The system was equipped with a 10x magnification cell (81 µm x 700 µm). Before each measurement, the cleanliness of the cell was checked visually. 200 µL of sample were used for the analysis and the images are collected with a flow rate of 0.15 mL/min, auto image frame rate of 29 frames/second and a sampling time of 74 seconds. The following settings were used for particle identification - 3 µm distance to the nearest neighbor, particle segmentation thresholds of 13 and 10 for the dark and light pixels respectively. The particle size was reported as the equivalent spherical diameter (ESD). The VisualSpreadsheet® 4.7.6 software was used for data collection and evaluation.

2.10. Reversed-Phase High-Performance Liquid Chromatography (RP-HPLC)

A Dionex Summit 2 system (Thermo Fisher, Dreieich, Germany) was used for the reversed-phase high-performance liquid chromatography. The samples were diluted to 0.1 g/L and 20 µL were injected on a BioBasic C18, 250 x 2.1, 5 µm column (Thermo Fisher, Dreieich, Germany). The sample elution was detected at 214 nm with a UVD170U UV/Vis detector (Thermo Fisher, Dreieich, Germany). A gradient of 32 to 48 % eluent B in A in 30 minutes was used. Eluent A consisted of 10 % w/v acetonitrile and 0.1 % w/v trifluoracetic acid in ultrapure water. Eluent B consisted of 0.1 % w/v trifluoracetic acid in acetonitrile. The flow rate was 0.2 mL/min. The column oven temperature was set at 30 ^{o}C. The chromatograms were integrated in Chromeleon V7 (Thermo Fisher, Dreieich, Germany) and the total relative area of all peaks different than the main peak (i.e. impurities) was calculated in percentage.

3. Results and Discussion

3.1. Formulation Step 1 – Studying the effect of solution pH on the thermal unfolding, aggregation and solubility of IFNα2a

In this work, we investigate a systematic sample-saving three-step approach to formulate a model protein. As a model protein, we use interferon alpha2a, a therapeutically-relevant molecule known to form aggregates that can cause clinical complications for the patients. During the first formulation step, we studied the effect of the pH on the solubility, thermal unfolding and aggregation of IFNα2a. To accomplish this, we used commercially available microdialysis devices, which allowed us to dialyse

small solution volume and test a wide range of pH values by consuming only a few micrograms of protein. The IFNα2a content in the supernatant after microdialysis against buffers with different pH was determined by UV spectrophotometry (i.e. with a NanoDrop 2000). The amount of soluble protein is lower at pH 6.0 and 6.5 as seen by the lower protein concentration and the lower fluorescence intensity in Figure 1. These observations are in a good agreement with the results reported by Sharma et al (Sharma and Kalonia, 2004). We also observed that the protein precipitates at pH 5.5 after gentle heating to 35-40 ^{o}C (data not shown). The low solubility of the protein in this pH range can be explained with the isoelectric point of IFNα2a which is around 6. It is common knowledge that the aqueous solubility of many proteins is reduced at pH values near the protein isoelectric point (Kantardjieff and Rupp, 2004). Based on these observations, we excluded the buffers with pH 5.5-6.5 from further studies.

Next, we used state-of-the-art microscale and microvolume approaches to study the unfolding, aggregation and the apparent hydrodynamic radius R_h of IFNα2a as a function of pH. With an increase of pH from 3.5 to 8.0 the protein unfolding transition becomes more cooperative (Figure 2A). The highest $IP_{350/330}$ is measured at pH 4.0 (Figure 2C). Between pH 4.5 and 8.0 the inflection points ($IP_{350/330}$) are around 66-67 ^{o}C. The lowest $IP_{350/330}$ is measured at pH 3.5 (Figure 2C). At pH 3.5 and 4.0 no aggregation during heating is detected with the aggregation detection optics, which indicates high colloidal stability of the protein in these conditions (Figure 2B). At pH 4.5 or higher, the samples start to form aggregates large enough to cause an increase in the signal of the aggregation detector of the Prometheus® NT.48, indicating lower protein colloidal stability (Figure 2B). The lowest aggregation temperature T_{agg} was measured at pH 5 (Figure 2C). At pH 4.5, 7.0, 7.5 and 8.0 IFNα2a shows similar T_{agg} around 65-66 ^{o}C (Figure 2C).

The apparent hydrodynamic radius of IFNα2a and the polydispersity of the samples measured with DLS is highly dependent on the solution pH. The R_h of IFNα2a is lower at pH 4.0 compared to the samples with a higher pH (Figure 2D). The highest R_h was measured in the pH range 7 to 8, which indicates that the protein probably forms oligomers in these conditions. Therefore, the pH range 7 to 8 was excluded from further studies. At pH 3.5 the DLS measurements indicated reproducibly that there is a population of larger particles in the samples. The latter is depicted by the high PDI at this pH. The apparent R_h and PDI derived from the cumulant fit for this condition are shown just for informational purpose. The change of the R_h during heating is also dependent on the pH (Figure 2E). At pH 4 the onset of aggregation T_{on} measured by DLS is around 60 ^{o}C and after the aggregates reach an R_h of about 30 nm, the aggregate growth stops (Figure 2E). The small aggregate size explains why no aggregation is detected with the Prometheus® NT.48 during heating of the IFNα2a samples with pH 4.0 (and pH 3.5). At higher pH (i.e. 4.5 and above) the T_{on} is shifted to a lower temperature and/or a

steep increase in the R_h without a plateau is observed (Figure 2E). The determined T_{on} values of IFNα2a with DLS are lowest at pH 4.5 and 5.0 (Figure 2F), which indicates lower protein colloidal stability in these conditions compared to pH 4.0. Important to note – only 150 µg of protein and less than 15 hours of total instrument measurement time per replicate were required to obtain the data for the entire pH screen presented in Figures 1 and 2.

As additional information for the readers we also compared the thermal unfolding of IFNα2a measured by the change of the intrinsic protein fluorescence intensity ratio (from the nanoDSF® measurement) and by the change in the protein ellipticity at 293 nm (from circular dichroism) and found excellent agreement between the two methods (Supplementary data – Figure S1.). Further, the inflection points from the change in the intrinsic protein fluorescence ratio during the thermal unfolding of IFNα2a at pH 5.0 correspond well with melting temperature of IFNa2a measured with differential scanning calorimetry (DSC) by Sharma et al.(Sharma and Kalonia, 2003). Noteworthy is that cuvette-based, DSC and near-UV CD devices do not allow the simultaneous thermal unfolding studies on many samples and require much more protein amount in comparison to the techniques we used in this study. Both nanoDSF® and DLS in micro well plates can be used to simultaneously measure dozens of samples.

3.2. Formulation Step 2 – Studying the effect of sodium chloride on the thermal unfolding and aggregation of IFNα2a

During the second formulation step, we focused on the effect of sodium chloride (i.e. ionic strength) on the stability of IFNα2a at pH 4.0 and pH 5.0. These two pH values were selected since IFNα2a shows very different behaviour – at pH 4.0 IFNα2a undergoes a less cooperative thermal unfolding but has high colloidal stability; at pH 5.0 the protein thermal unfolding is characterized by a sharp transition, but the protein colloidal stability is low.

Increasing the sodium chloride concentration from 0 to 120 mM causes a shift in the unfolding transitions of IFNα2a to a lower temperature (Figure 3A and 3D). This shift is more pronounced at pH 4 (compared to pH 5) where the $IP_{350/330}$ is around 72-73 ^{o}C without sodium chloride and around 61 ^{o}C in the presence of 120 mM NaCl (Figure 3C). This indicates that the addition of sodium chloride has a very unfavourable effect on the protein thermal stability at pH 4.0. For comparison, at pH 5.0 the difference in the $IP_{350/330}$ with 0 mM or with 120 mM sodium chloride is only 1.5-2 ^{o}C (Figure 3F).

The addition of 30 mM or more sodium chloride to the 10 mM sodium acetate buffer with pH 4 results in IFNα2a aggregation (i.e. larger aggregates) during heating, which is detectable by the Prometheus® NT.48 (Figure 3B). An increase in the NaCl concentration from 30 mM to 120 mM shifts the T_{agg} in the samples with pH 4 to lower temperatures (Figure 3C). At pH 5, the sodium chloride has a small

influence on the aggregation of IFNα2a during heating and 120 mM NaCl reduce the T_{agg} with only approximately 2 ^{o}C (Figure 3E and 3F).

At pH 4.0 the protein R_h from DLS increases with the addition of only 10-20 mM NaCl and does not change when the salt concentration is further increased (Figure 4A). At pH 5.0 the R_h decreases slightly with increasing NaCl concentration (Figure 4A). At pH 4.0 the addition of NaCl greatly shifts the protein T_{on} to lower temperatures (Figure 4B) and causes the formation of larger aggregates during heating (Figure 4C). At pH 5.0 the increasing sodium chloride concentration causes only a moderate decrease in the IFNα2a T_{on} (Figure 4B) and does not affect the steepness of the increase in the protein R_h during heating (Figure 4D). These observations are in a good agreement with the data in Figure 3B and 3E. Once again, it is important to mention that all the data presented in Figures 3 and 4 was obtained with the consumption of 300 µg of protein and less than 15 hours of measurement time per replicate.

3.3. Formulation Step 3 - Advanced structural characterization of IFNα2a

3.3.1. Effect of the pH on the conformational stability of IFNα2a

Interferon alpha2a shows a two-state unfolding behaviour in an isothermal chemical denaturation experiment with guanidine hydrochloride (Figure 5). The calculated Gibbs free energy of unfolding ΔG is lower (mean value of 29.45 kJ/mol) at pH 4 compared to the ΔG at pH 5 (mean value of 40.53 kJ/mol), although the melting denaturant concentration C_m is higher (mean value of 4.5 M GuHCl) at pH 4 compared to pH 5 (mean value of 4.01 M GuHCl). The reason for the lower ΔG at the lower pH is the lower m-value at pH 4 compared to pH 5, which indicates a less cooperative unfolding of IFNα2a in this condition. According to the ΔG, IFNα2a has lower conformational stability at pH 4.0 compared to pH 5.0. Noteworthy is that the dG, C_m and m-value that were determined at pH 5.0 are in excellent agreement with the values reported by Bis et al.(Bis et al., 2015). Another interesting observation is that the unfolding behaviour (regarding cooperativity and the position of the inflection point) of IFNα2a at pH 4 and 5 during heating resembles the unfolding of the protein in guanidine hydrochloride (Figure 2A and Figure 5). Only 240 µg of protein were required to obtain one isothermal chemical denaturation graph containing 24 points like the graphs depicted in Figure 5.

3.3.2. Effect of pH and sodium chloride on the secondary and tertiary structure of IFNα2a

The amide I band of IFNα2a shows a maximum between 1650 and 1655 cm^{-1} at both pH 4 and pH 5 with or without 70 mM sodium chloride (Figure 6A). This corresponds well to alpha-helical secondary protein structure which is expected for this protein and is also consistent with previously published data(Bis et al., 2015; Sharma and Kalonia, 2004; van de Weert and Jørgensen, 2012). Additionally, the characteristic far-UV CD spectra with two minima at 209 and 222 nm confirm the presence of alpha-helical protein structure in all four conditions (Figure 6B)(Johnson, 1990). The near-UV CD spectra of

IFNα2a in 10 mM Na-acetate pH 4 or 5 with or without 70 mM NaCl show the typical negative peaks at 287 nm and 293 nm which are assigned to the two tryptophan residues of this protein(Sharma and Kalonia, 2004, 2003). This indicates that the tertiary structure of IFNα2a is the same in the four formulation conditions tested. Noteworthy, both CD and FTIR are non-destructive methods in the way we used them, and the sample was recovered after the measurements.

3.4. Long-term storage stability of IFNα2a

3.4.1. Formation of small soluble aggregates detected by HP-SEC

The stock solution of IFNα2a contains approximately 1 % high molecular weight species (i.e. small soluble aggregates) detectable by HP-SEC already after thawing. After dialysis against acetate buffer with pH 5.0 these aggregates remain in the solution, while after dialysis in the buffer with pH 4.0 these aggregates are no longer present (Figure 7). The latter was already observed during formulation/deformulation of IFNα2a(Panjwani et al., 2010). After storage of the samples at 25 ^{o}C up to 12 months, the relative area of small soluble aggregates increases more at pH 5.0 compared to the samples with pH 4.0 (Figure 7A). This is in a good agreement with the results from the biophysical characterisation which shows that both the thermal and colloidal stability of IFNα2a is higher in 10 mM Na-acetate with pH 4 compared to pH 5. Interestingly, the addition of 70 mM sodium chloride seems to play a small role in the presence of the small soluble aggregates of IFNα2a at both pH 4.0 and pH 5.0 (Figure 7A), although it affected the aggregation behaviour of the protein in the short-term characterisation (Figures 3 and 4). During storage at 4 ^{o}C no increase in the amount of small soluble aggregates was observed, although the samples with pH 5.0 contain more aggregates during the entire stability study compared to the samples with pH 4.0 (Figure 7B). For a sample chromatogram from the HP-SEC method see Figure S2 in the supplementary data.

3.4.2. Formation of larger protein aggregates (sub-visible particles)

The highest numbers of particles in all three size ranges were measured in IFNα2a formulations with 70 mM sodium chloride after storage at 25 ^{o}C (Figure 8 – Above). This is in a good agreement with the earlier observations that the addition of sodium chloride causes the formation of larger aggregates at pH 4 and reduces the thermal and colloidal protein stability (Figures 3 and 4). Both formulations with only 10 mM Na-acetate and no sodium chloride contain a very low number of particles after storage at 25 ^{o}C (Figure 8 – Above). Still, the formulation at pH 4.0 without NaCl contains fewer particles (specifically in the size range 10 to 25 µm and above 25 µm) compared to pH 5.0 without NaCl.

During storage at 4 ^{o} C fewer particles are formed compared to storage at 25 ^{o}C (Figure 8). After storage at 4 ^{o}C the IFNα2a formulation containing the highest number of particles of any size is with 10 mM Na-acetate pH 5.0 and 70 mM sodium chloride. The formulation containing only 10 mM Na-acetate at

pH 4.0 without sodium chloride shows the lowest particle numbers after storage at both 4 and 25 °C (Figure 8). Important to note, this is the condition in which IFNα2a has the highest $IP_{350/330}$ (Figure 2C), a high T_{on} (Figure 2F), small aggregate size after heating (Figure 2E) and a low R_h and PDI at 25 °C (Figure 2D).

3.4.3. Formation of impurities detected by RP-HPLC

Although the chemical protein degradation is a topic outside the scope of this article, we wanted to study if there are differences in the chemical degradation of IFNα2a during storage at pH 4 and pH 5 with or without sodium chloride. We selected RP-HPLC as a well-established technique to detect chemically changed species of IFNα2a(Hermeling et al., 2005; Mohl and Winter, 2006; Sharma and Kalonia, 2004). For a sample RP-HPLC chromatogram from the method we used see Figure S3 in the supplementary data. More chemically changed species (i.e. impurities) detected by RP-HPLC form during storage at 25 °C compared to storage at 4 °C (Figure 9). However, the relative area of impurities formed (and the retention time of the impurity peaks) were the same at both pH 4.0 and pH 5.0, regardless of the presence/absence of 70 mM sodium chloride. These results indicate that the chemical changes of IFNα2a that occur during long-term storage in the four conditions tested in Figure 9 are similar and the differences in the protein degradation in these conditions are driven by the different conformational and/or colloidal protein stability. Although, the chemical changes are not directly assessed by the "1-2-3 Step" protein formulation approach, one could additionally perform short-term stress tests (i.e. high temperature, light exposure) coupled to a suitable analytical technique on the formulations in Step 2 to get complementary data whether a difference in the chemical stability of the lead formulations is expected(Manning et al., 2018, 2010).

3.4.4. Is there a correlation between the rapid sample-saving biophysical characterization and the long-term stability data?

The aggregation of a protein can be augmented by low conformational and/or low colloidal protein stability, both of which could be influenced by pH and/or ionic strength(E. Y. Chi et al., 2003; E. Y. E. Chi et al., 2003). Interferon alpha2a has lower conformational stability and shows less cooperative thermal and GuHCl-induced unfolding at pH 4.0 compared to pH 5.0. However, at low ionic strength in 10 mM sodium acetate, the colloidal stability of IFNα2a is higher at pH 4 than at pH 5. This is in excellent agreement with the less small and large protein aggregates formed during storage of IFNα2a at 25 °C and 4 °C at pH 4 without sodium chloride, which indicates that the high colloidal stability is crucial to obtain a stable IFNα2a formulation. The addition of sodium chloride (i.e. an increase of ionic strength) has a negative effect on the protein colloidal stability (depicted by a reduction of the T_{agg}, T_{on} and an

increase in the aggregate size formed during heating), which also corresponds well with the formation of large protein aggregates during storage of IFNα2a in solutions containing 70 mM sodium chloride.

4. Conclusion

In this work, we demonstrated how some of the contemporary tools for protein characterisation can be used to perform quick and less-sample-demanding formulation studies on interferon alpha2a, studied at protein concentrations significantly higher than used in commercial formulations. We structured these studies in a 3-step formulation approach, including Step 1 - Screen for optimal pH; Step 2 - Screen for the effect of ionic strength (i.e. sodium chloride) on the protein stability; Step 3 - Advanced structural characterization; We validated the results from the rapid biophysical protein characterisation by performing long-term stability studies at 4 °C and 25 °C during which we studied the formation of small and large aggregates of IFNα2a. Both the rapid sample-saving biophysical characterisation and the long-term stability data indicate that the aggregation of interferon alpha2a is minimal in 10 mM sodium acetate buffer with pH 4. The addition of sodium chloride (i.e. an increase of ionic strength) to IFNα2a solutions has a negative effect on the protein physical stability. The presented work is important in several directions – First, it shows that thanks to technological advancement we can nowadays perform quick systematic formulation studies with miniature samples amounts. Second, it shows that the rapid sample-saving techniques we apply here were indeed able to find an interferon alpha2a formulation that is very stable during long-term storage. Third, the work reveals new insights into the stability of interferon alpha2a in different conditions. Finally, it shows that the proposed combination of sample-saving techniques could significantly and quickly reduce the number of formulations that will move to accelerated and/or long-term stability studies and therefore reduce development costs and time dramatically.

Acknowledgements

This study was funded by a project part of the EU Horizon 2020 Research and Innovation programme under the Marie Skłodowska-Curie grant agreement No 675074.

References

Baron, S., Tyring, S.K., Fleischmann, W.R., Coppenhaver, D.H., Niesel, D.W., Klimpel, G.R., Stanton, G.J., Hughes, T.K., 1991. The Interferons. JAMA 266, 1375. https://doi.org/10.1001/jama.1991.03470100067035

Bessa, J., Boeckle, S., Beck, H., Buckel, T., Schlicht, S., Ebeling, M., Kiialainen, A., Koulov, A., Boll, B.,

Weiser, T., Singer, T., Rolink, A.G., Iglesias, A., 2015. The Immunogenicity of Antibody Aggregates in a Novel Transgenic Mouse Model. Pharm. Res. 32, 2344–2359. https://doi.org/10.1007/s11095-015-1627-0

Bis, R.L., Singh, S.M., Cabello-Villegas, J., Mallela, K.M.G., 2015. Role of benzyl alcohol in the unfolding and aggregation of interferon α-2a. J. Pharm. Sci. 104, 407–415. https://doi.org/10.1002/jps.24105

Boll, B., Bessa, J., Folzer, E., Ríos Quiroz, A., Schmidt, R., Bulau, P., Finkler, C., Mahler, H.-C., Huwyler, J., Iglesias, A., Koulov, A. V., 2017. Extensive Chemical Modifications in the Primary Protein Structure of IgG1 Subvisible Particles Are Necessary for Breaking Immune Tolerance. Mol. Pharm. 14, 1292–1299. https://doi.org/10.1021/acs.molpharmaceut.6b00816

Brader, M.L., Estey, T., Bai, S., Alston, R.W., Lucas, K.K., Lantz, S., Landsman, P., Maloney, K.M., 2015. Examination of thermal unfolding and aggregation profiles of a series of developable therapeutic monoclonal antibodies. Mol. Pharm. 12, 1005–1017. https://doi.org/10.1021/mp400666b

Braun, A., Kwee, L., Labow, M.A., Alsenz, J., 1997. Protein Aggregates Seem to Play a Key Role Among the Parameters Influencing the Antigenicity of Interferon Alpha (IFN-α) in Normal and Transgenic Mice. Pharm. Res. 14, 1472–1478. https://doi.org/10.1023/A:1012193326789

Chi, E.Y., Krishnan, S., Randolph, T.W., Carpenter, J.F., 2003. Physical stability of proteins in aqueous solution: Mechanism and driving forces in nonnative protein aggregation. Pharm. Res. 20, 1325–1336. https://doi.org/10.1023/A:1025771421906

Chi, E.Y.E., Krishnan, S., Kendrick, B.S.B.B.S., Chang, B.S., Carpenter, J.F., Randolph, T.W., 2003. Roles of conformational stability and colloidal stability in the aggregation of recombinant human granulocyte colony-stimulating factor. Protein Sci. 12, 903–913. https://doi.org/10.1110/ps.0235703.mer

Diress, A., Lorbetskie, B., Larocque, L., Li, X., Alteen, M., Isbrucker, R., Girard, M., 2010. Study of aggregation, denaturation and reduction of interferon alpha-2 products by size-exclusion high-performance liquid chromatography with fluorescence detection and biological assays. J. Chromatogr. A 1217, 3297–3306. https://doi.org/10.1016/j.chroma.2009.10.081

Dragomiretskaya, N., Izha, A., Kalinichenko, N., Szark-Eckardt, M., Klimczyk, M., Cieślicka, M., Muszkieta, R., Prusik, K., Napierała, M., Żukowska, H., Zukow, W., 2015. Use of antiviral therapy in patients with chronic hepatitis C. Open Med. (Warsaw, Poland) 10, 209–215. https://doi.org/10.1515/med-2015-0032

Escudier, B., Pluzanska, A., Koralewski, P., Ravaud, A., Bracarda, S., Szczylik, C., Chevreau, C., Filipek, M., Melichar, B., Bajetta, E., Gorbunova, V., Bay, J.-O., Bodrogi, I., Jagiello-Gruszfeld, A., Moore, N., 2007. Bevacizumab plus interferon alfa-2a for treatment of metastatic renal cell carcinoma: a randomised, double-blind phase III trial. Lancet 370, 2103–2111. https://doi.org/10.1016/S0140-6736(07)61904-7

Goldberg, D.S., Lewus, R.A., Esfandiary, R., Farkas, D.C., Mody, N., Day, K.J., Mallik, P., Tracka, M.B., Sealey, S.K., Samra, H.S., 2017. Utility of High Throughput Screening Techniques to Predict Stability of Monoclonal Antibody Formulations During Early Stage Development. J. Pharm. Sci. 106, 1971–1977. https://doi.org/10.1016/j.xphs.2017.04.039

Hermeling, S., Aranha, L., Mirjam Damen, J.A., Slijper, M., Schellekens, H., Crommelin, D.J., Jiskoot, W., 2005. Chapter 6 Structural characterization and immunogenicity in wildtype and immune tolerant mice of degraded recombinant human interferon alpha2b, Pharmaceutical Research.

Hochuli, E., 1997. Interferon immunogenicity: technical evaluation of interferon-alpha 2a. J. Interferon Cytokine Res. 17 Suppl 1, S15-21.

ICH, Q5C Quality of Biotechnological Products: Stability Testing of Biotechnological/Biological Products, 1995. . Geneva.

Johnson, W.C., 1990. Protein secondary structure and circular dichroism: A practical guide. Proteins Struct. Funct. Genet. 7, 205–214. https://doi.org/10.1002/prot.340070302

Jonasch, E., Haluska, F.G., 2001. Interferon in oncological practice: review of interferon biology, clinical applications, and toxicities. Oncologist 6, 34–55. https://doi.org/10.1634/THEONCOLOGIST.6-1-34

Kantardjieff, K.A., Rupp, B., 2004. Protein isoelectric point as a predictor for increased crystallization screening efficiency. Bioinforma. Discov. NOTE 20, 2162–2168. https://doi.org/10.1093/bioinformatics/bth066

Linke, P., Amaning, K., Maschberger, M., Vallee, F., Steier, V., Baaske, P., Duhr, S., Breitsprecher, D., Rak, A., 2016. An Automated Microscale Thermophoresis Screening Approach for Fragment-Based Lead Discovery. J. Biomol. Screen. 21, 414–21. https://doi.org/10.1177/1087057115618347

Manning, M.C., Chou, D.K., Murphy, B.M., Payne, R.W., Katayama, D.S., 2010. Stability of protein pharmaceuticals: An update. Pharm. Res. 27, 544–575. https://doi.org/10.1007/s11095-009-0045-6

Manning, M.C., Liu, J., Li, T., Holcomb, R.E., 2018. Rational Design of Liquid Formulations of Proteins, Advances in Protein Chemistry and Structural Biology. Academic Press. https://doi.org/10.1016/bs.apcsb.2018.01.005

Mohl, S., Winter, G., 2006. Continuous Release of rh-Interferon α-2a from Triglyceride Implants: Storage Stability of the Dosage Forms. Pharm. Dev. Technol. 11, 103–110. https://doi.org/10.1080/10837450500464230

Moussa, E.M., Panchal, J.P., Moorthy, B.S., Blum, J.S., Joubert, M.K., Narhi, L.O., Topp, E.M., 2016. Immunogenicity of Therapeutic Protein Aggregates. J. Pharm. Sci. 105, 417–430. https://doi.org/10.1016/J.XPHS.2015.11.002

Narhi, L.O., Schmit, J., Bechtold-Peters, K., Sharma, D., 2012. Classification of Protein Aggregates, J Pharm Sci.

Panjwani, N., Hodgson, D.J., Sauvé, S., Aubin, Y., 2010. Assessment of the Effects of pH, Formulation and Deformulation on the Conformation of Interferon Alpha-2 by NMR. J. Pharm. Sci. 99, 3334–3342. https://doi.org/10.1002/jps.22105

Ratanji, K.D., Derrick, J.P., Dearman, R.J., Kimber, I., 2014. Immunogenicity of therapeutic proteins: Influence of aggregation. J. Immunotoxicol. 11, 99–109. https://doi.org/10.3109/1547691X.2013.821564

Revers, L., Furczon, E., 2010. An Introduction to Biologics and Biosimilars. Part I: Biologics: What are They and Where Do They Come from? Can. Pharm. J. / Rev. des Pharm. du Canada 143, 134–139. https://doi.org/10.3821/1913-701X-143.3.134

Roberts, C.J., 2007. Non-Native Protein Aggregation Kinetics. Springer New York, New York, NY.

Roberts, C.J., Das, T.K., Sahin, E., 2011. Predicting solution aggregation rates for therapeutic proteins: Approaches and challenges. Int. J. Pharm. 418, 318–333. https://doi.org/10.1016/j.ijpharm.2011.03.064

Robinson, M.J., Matejtschuk, P., Bristow, A.F., Dalby, P.A., 2018. Tm-Values and Unfolded Fraction Can Predict Aggregation Rates for Granulocyte Colony Stimulating Factor Variant Formulations but Not under Predominantly Native Conditions. Mol. Pharm. 15, 256–267. https://doi.org/10.1021/acs.molpharmaceut.7b00876

Rosenberg, A.S., 2006. Effects of protein aggregates: An immunologic perspective. AAPS J. 8, E501–E507. https://doi.org/10.1208/aapsj080359

Savitzky, A., E, M.J., 1951. Smoothing and Differentiation of Data by Simplified Least Squares

Procedures, Z. Physiol. Chem.

Sharma, V.K., Kalonia, D.S., 2004. Polyethylene glycol-induced precipitation of interferon alpha-2a followed by vacuum drying: Development of a novel process for obtaining a dry, stable powder. AAPS J. 6, 31–44. https://doi.org/10.1208/ps060104

Sharma, V.K., Kalonia, D.S., 2003. Temperature- and pH-Induced Multiple Partially Unfolded States of Recombinant Human Interferon- 2a: Possible Implications in Protein Stability. Pharm. Res. 20, 1721–1729. https://doi.org/10.1023/B:PHAM.0000003367.62900.0f

Smith, N., Mori, S. a, Henderson, A., 2010. Aggregation of Therapeutic Proteins. John Wiley & Sons, Inc., Hoboken, New Jersey.

Söltl, F., Derix, J., Blech, M., Breitsprecher, D., 2015. Analysis of formulation-dependent colloidal and conformational stability of monoclonal antibodies. Appl. Note NT-PR-005 1.

Svilenov, H., Markoja, U., Winter, G., 2018. Isothermal chemical denaturation as a complementary tool to overcome limitations of thermal differential scanning fluorimetry in predicting physical stability of protein formulations. Eur. J. Pharm. Biopharm. 125, 106–113. https://doi.org/10.1016/j.ejpb.2018.01.004

Towsend, R., Kumosisski, T.F., Timasheff, S.N., 1967. The Circular Dichroism of Variants of P-Lactoglobulin, THE JOURNAL cm RIOLOGICAL CHEMISTRY.

US5762923A - Stabilized interferon alpha solutions - Google Patents [WWW Document], n.d. URL https://patents.google.com/patent/US5762923A/en?q=interferon&q=alpha (accessed 8.7.18).

van de Weert, M., Jørgensen, L., 2012. Infrared Spectroscopy to Characterize Protein Aggregates, in: Analysis of Aggregates and Particles in Protein Pharmaceuticals. John Wiley & Sons, Inc., Hoboken, NJ, USA, pp. 227–248. https://doi.org/10.1002/9781118150573.ch10

Wang, W., Roberts, C.J., 2018. Protein Aggregation - Mechanisms, Detection, and Control. Int. J. Pharm. https://doi.org/10.1016/J.IJPHARM.2018.08.043

Wanner, R., Breitsprecher, D., Duhr, S., Baaske, P., Winter, G., 2017. Thermo-Optical Protein Characterization for Straightforward Preformulation Development. J. Pharm. Sci. 106, 2955–2958. https://doi.org/10.1016/j.xphs.2017.06.002

Figure legend

Figure 1. Effect of the pH on the concentration and the intrinsic fluorescence of IFNα2a in the supernatant after microdialysis. The values are mean of triplicates, the bars show the standard deviation.

Figure 2. Effect of pH on IFNα2a unfolding and aggregation – Above: Thermal unfolding traces (A) and scattering traces (B) with the corresponding inflection points (IP350/330) and aggregation onset temperatures (Tagg) (C) measured with nanoDSF®; Below: The apparent hydrodynamic radius and PDI (D), the temperature dependence of the R_h (E) and the calculated aggregation onset temperatures from DLS (F). The values in (D) are means of triplicates, the bars show the standard deviation. In (C) and (F) the value from each triplicate is shown.

Figure 3. nanoDSF® evaluation of the effect of sodium chloride on IFNα2a – thermal unfolding traces at pH 4 (A) and pH 5 (D), scattering traces from the aggregation detection optics at pH 4 (B) and pH 5 (E) and the corresponding inflection points and aggregation temperatures at pH 4 (C) and pH 5 (F). In (C) and (F) the value from each triplicate is shown.

Figure 4. Effect of sodium chloride on: the apparent hydrodynamic radius R_h from DLS of IFNα2a at pH 4 and pH 5 (A); the aggregation onset temperature of IFNα2a from DLS at pH 4 and pH 5 (B); the temperature dependence of the R_h from DLS of IFNα2a at pH 4 (C) and pH 5 (D). In (A) and (B) the values from each triplicate is shown.

Figure 5. Isothermal chemical denaturation of IFNα2a with guanidine hydrochloride in 10 mM sodium acetate buffer with pH 4 and pH 5. The values from each triplicate are shown. The table in the inset shows the calculated means and standard deviations for the ΔG, C_m and m-value from the two-state unfolding fit.

Figure 6. Effect of pH and 70 mM sodium chloride on: the secondary structure of IFNα2a studied by FTIR (A) and far-UV circular dichroism (B); and the tertiary structure of IFNa2a studied by near-UV circular dichroism (C);

Figure 7. Small soluble aggregates (high molecular weight species) of IFNα2a measured with HP-SEC during long-term storage of the samples at 25 ^{o}C (A) and 4 ^{o}C (B). The values are mean of triplicates from three different vials, the bars show the standard deviation.

Figure 8. Subvisible particles detected with flow imaging microscopy in IFNα2a solutions during storage at 25 ^{o}C (above) and 4 ^{o}C (below). The values are mean of triplicates from three different vials, the bars show the standard deviation.

Figure 9. Relative area of all impurities detected by RP-HPLC in IFNα2a solutions during storage at 25 ^{o}C (A) and 4 ^{o}C (B). The values are mean of triplicates from three different vials, the bars show the standard deviation.

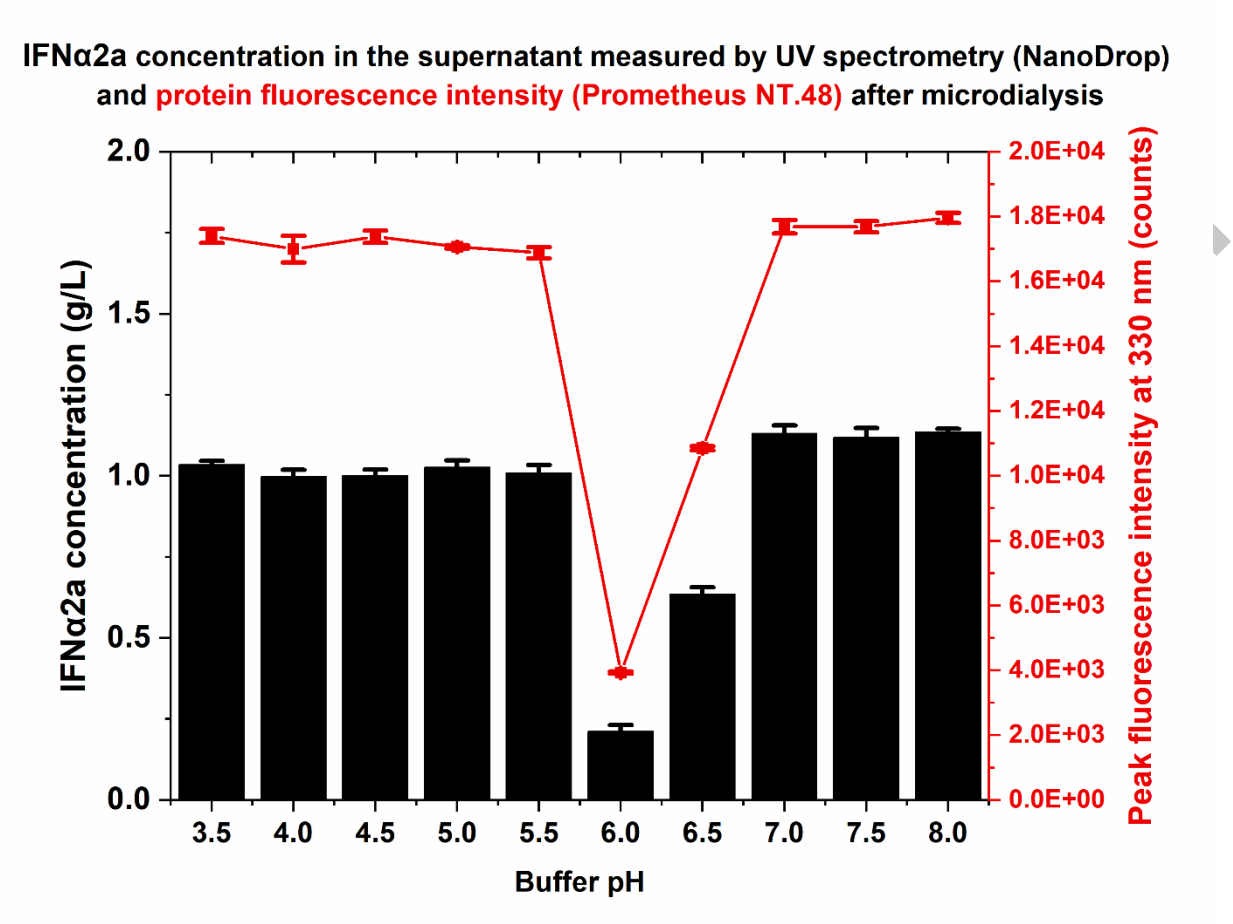
IFNα2a concentration in the supernatant measured by UV spectrometry (NanoDrop)
and protein fluorescence intensity (Prometheus NT.48) after microdialysis
IFNα2a concentration (g/L)
Peak fluorescence intensity at 330 nm (counts)
Buffer pH

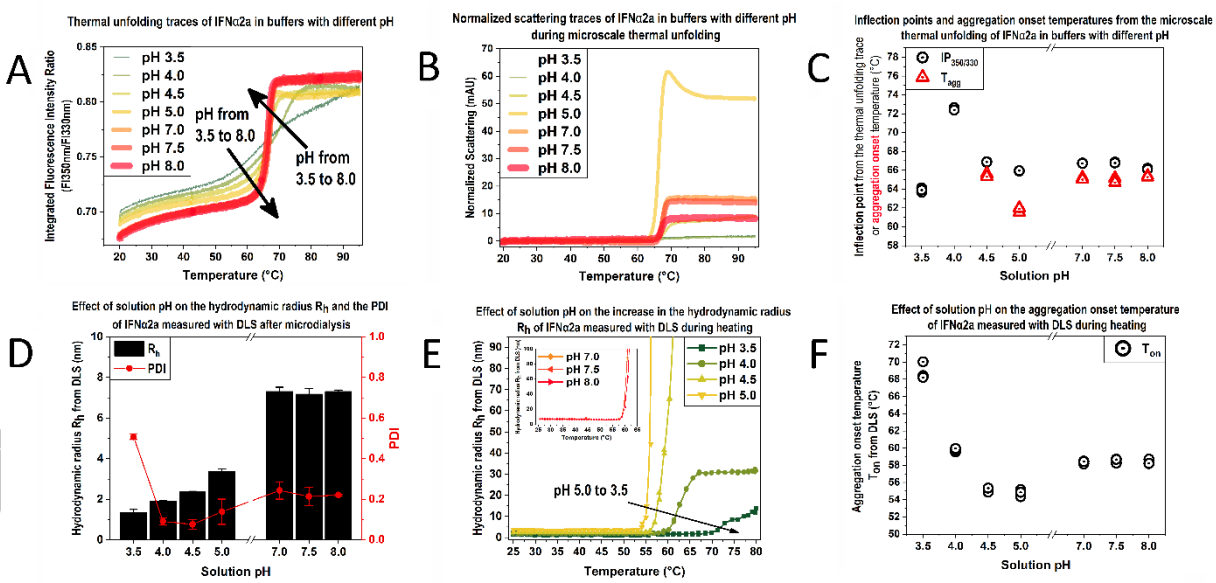
A
Thermal unfolding traces of IFNα2a in buffers with different pH
Integrated Fluorescence Intensity Ratio (F350nm/F330nm)
pH 3.5
pH 4.0
pH 4.5
pH 5.0
pH 7.0
pH 7.5
pH 8.0
pH from 3.5 to 8.0
pH from 3.5 to 8.0
Temperature (°C)
B
Normalized scattering traces of IFNα2a in buffers with different pH during microscale thermal unfolding
Normalized Scattering (mAU)
Temperature (°C)
C
Inflection points and aggregation onset temperatures from the microscale thermal unfolding of IFNα2a in buffers with different pH
Inflection point from the thermal unfolding trace or aggregation onset temperature (°C)
Solution pH
D
Effect of solution pH on the hydrodynamic radius Rh and the PDI of IFNα2a measured with DLS after microdialysis
Hydrodynamic radius Rh from DLS (nm)
PDI
Solution pH
E
Effect of solution pH on the increase in the hydrodynamic radius Rh of IFNα2a measured with DLS during heating
Hydrodynamic radius Rh from DLS (nm)
pH 5.0 to 3.5
Temperature (°C)
F
Effect of solution pH on the aggregation onset temperature of IFNα2a measured with DLS during heating
Aggregation onset temperature Ton from DLS (°C)
Solution pH

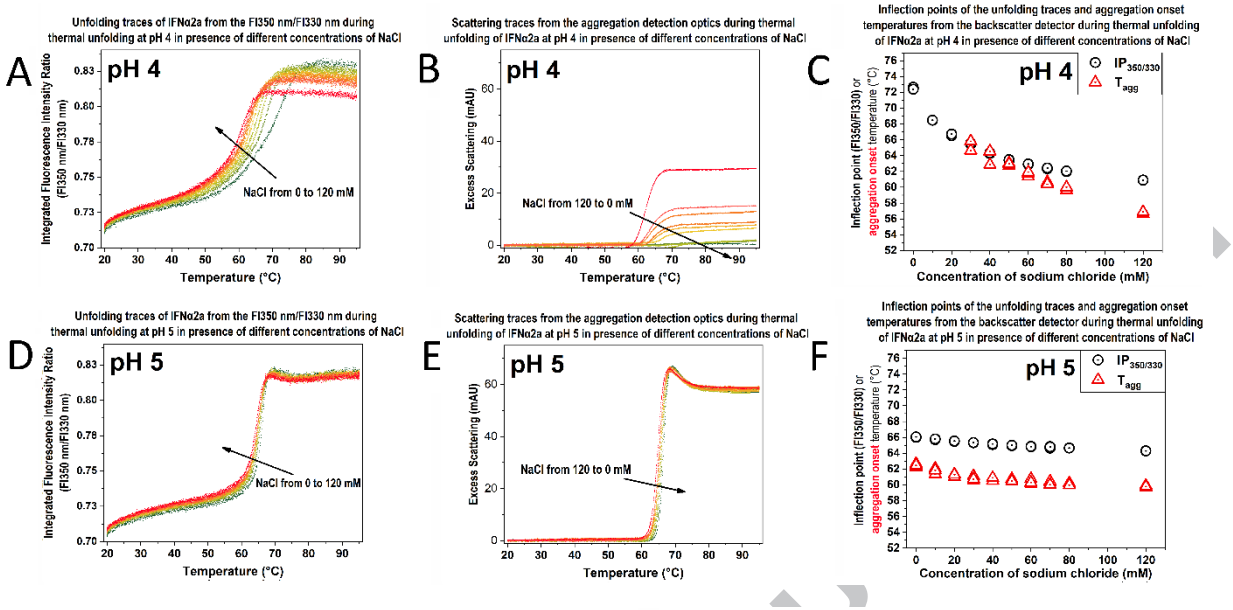

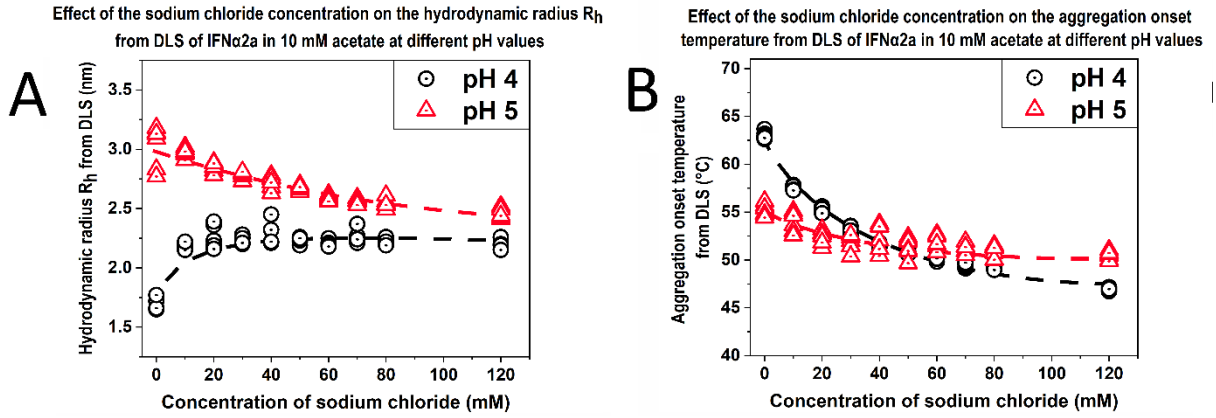

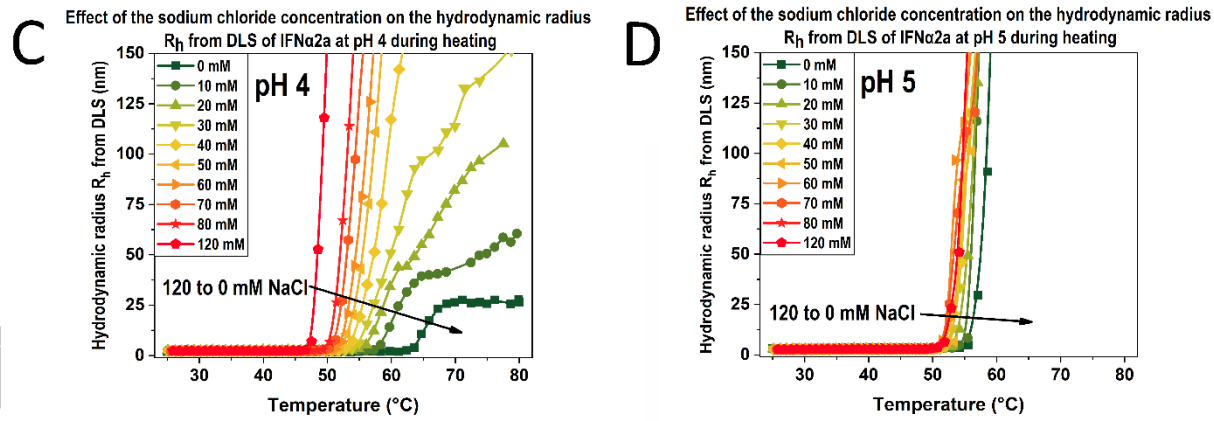

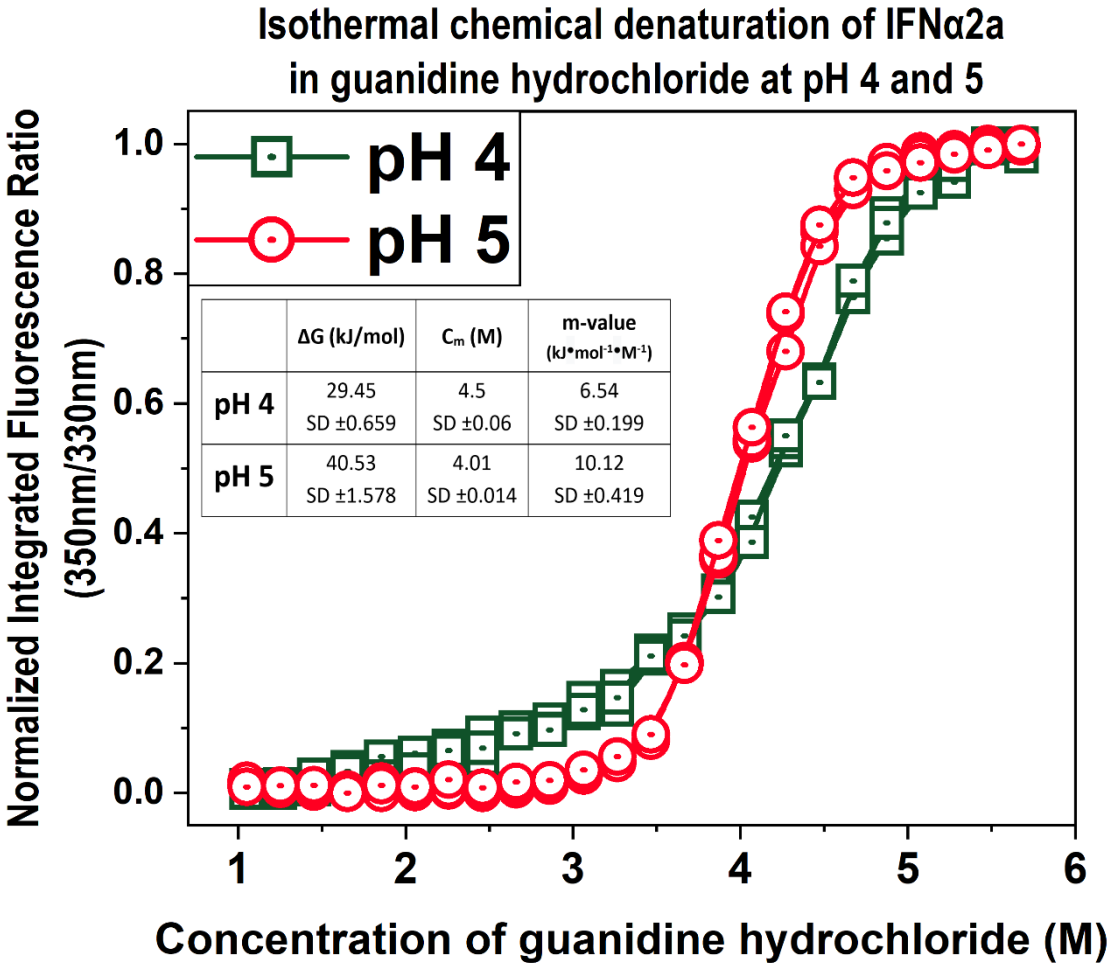
Isothermal chemical denaturation of IFNα2a
in guanidine hydrochloride at pH 4 and 5
pH 4
pH 5
Normalized Integrated Fluorescence Ratio
(350nm/330nm)
Concentration of guanidine hydrochloride (M)
ΔG (kJ/mol)
Cm (M)
m-value
(kJ•mol-1•M-1)
pH 4
29.45
SD ±0.659
4.5
SD ±0.06
6.54
SD ±0.199
pH 5
40.53
SD ±1.578
4.01
SD ±0.014
10.12
SD ±0.419

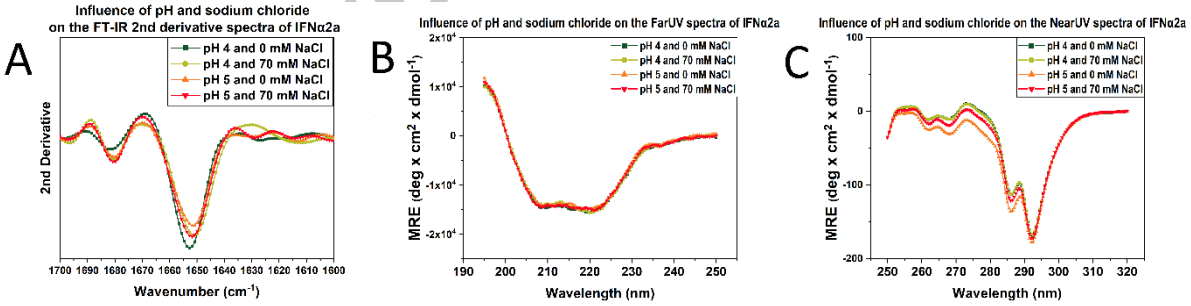
A
Influence of pH and sodium chloride
on the FT-IR 2nd derivative spectra of IFNα2a
pH 4 and 0 mM NaCl
pH 4 and 70 mM NaCl
pH 5 and 0 mM NaCl
pH 5 and 70 mM NaCl
2nd Derivative
Wavenumber (cm-1)
B
Influence of pH and sodium chloride on the FarUV spectra of IFNα2a
MRE (deg x cm2 x dmol-1)
Wavelength (nm)
C
Influence of pH and sodium chloride on the NearUV spectra of IFNα2a
MRE (deg x cm2 x dmol-1)
Wavelength (nm)

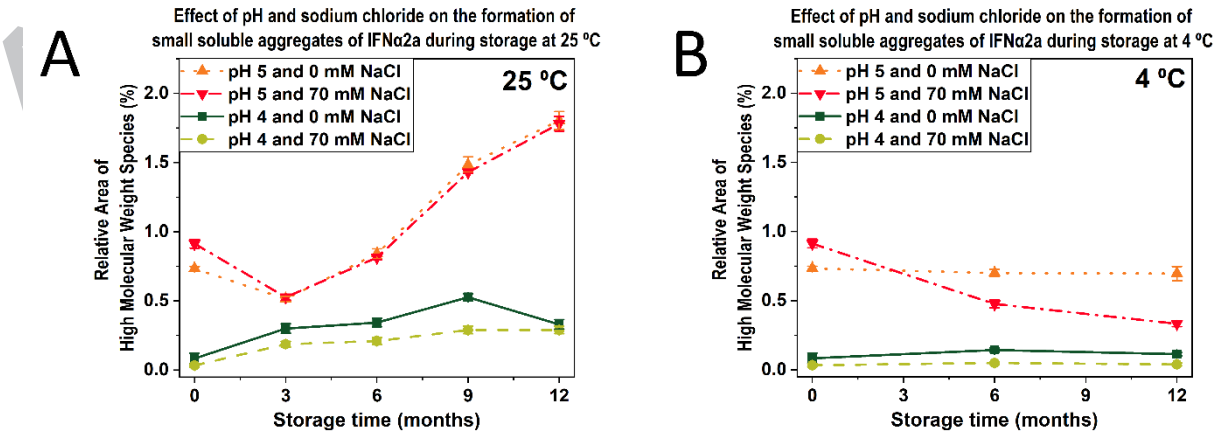
A
Effect of pH and sodium chloride on the formation of
small soluble aggregates of IFNα2a during storage at 25 ºC
pH 5 and 0 mM NaCl
pH 5 and 70 mM NaCl
pH 4 and 0 mM NaCl
pH 4 and 70 mM NaCl
25 ºC
Relative Area of
High Molecular Weight Species (%)
Storage time (months)
B
Effect of pH and sodium chloride on the formation of
small soluble aggregates of IFNα2a during storage at 4 ºC
4 ºC